BJR

https://doi.org/10.1259/bjr.20180075

Received: 15 January 2018 | Revised: 27 March 2019 | Accepted: 01 April 2019

Cite this article as:
Lee S-M, Wolfe K, Acher P, Liyanage SH. Multiparametric MRI appearances of primary granulomatous prostatitis. *Br J Radiol* 2019; **92**: 20180075.

FULL PAPER

Multiparametric MRI appearances of primary granulomatous prostatitis

[1]SU-MIN LEE, PhD MRCS, [2]KONRAD WOLFE, MBChB, [3]PETER ACHER, PhD FRCS and [4]SIDATH H LIYANAGE, MBBS

[1]Department of Urology, Bristol Urological Institute, Southmead Hospital, Bristol, UK
[2]Department of Pathology, Southend University Hospital, Westcliff-on-Sea, Essex, UK
[3]Department of Urology, Southend University Hospital, Westcliff-on-Sea, Essex, UK
[4]Department of Radiology, Southend University Hospital, Westcliff-on-Sea, Essex, UK

Address correspondence to: Mr Su-Min Lee
E-mail: *smlee84@gmail.com*

Objective: Radiological features of granulomatous prostatitis (GP) overlap with those of prostate adenocarcinoma. Identification of specific GP features may aid diagnosis. We aimed to evaluate the multiparametric MRI (mpMRI) features of GP.
Methods: We retrospectively reviewed 16 patients from a cohort undergoing mpMRI and transperineal sector-guided prostate biopsies between July 2012 and May 2017. Images were analysed for lesion location, shape, size, extracapsular extension, signal intensity (SI), apparent diffusion coefficient (ADC) values, dynamic contrast enhancement (DCE) pattern and PI-RADS (Prostate Imaging – Reporting and Data System) v2 score.
Results: Histology revealed 13 cases of nonspecific GP and 3 cases of xanthogranulomatous prostatitis. GP lesions were diffuse involving > 50% of the prostate (n = 13) or nodular (n = 3). Signal intensity on T_2 weighted imaging was low and high on diffusion-weighted imaging. ADC values were low (mean 702 ± 79 × 10^{-6} mm/s^2). Five patients had DCE imaging with all cases 'positive' as per PI-RADS scoring, with two cases displaying further ring enhancement consistent with abscess formation. Overall PI-RADS score for all cases was 5, indicating high suspicion of prostate cancer.
Conclusion: GP is difficult to differentiate from prostate cancer, but typically gives diffuse changes involving > 50% of the gland on mpMRI, with extracapsular extension and rim-enhancing areas. It should be considered a differential diagnosis in patients with recent urinary tract infection (UTI) or prior Bacillus Calmette-Guerin (BCG) treatment.
Advances in knowledge: Prostate MRI imaging features including diffuse changes, extracapsular extension and rim-enhancing areas, in patients with recent UTI or BCG treatment may help identify granulomatous prostatitis cases.

INTRODUCTION

Multiparametric MRI (mpMRI) for pre-biopsy diagnosis and staging of prostate cancer is increasing.[1] It allows for identification and targeting of suspicious lesions, improving the detection rate of significant tumours and providing more accurate evaluation of overall tumour burden.[2] Furthermore, mpMRI may help avoid biopsy in some males, as well as playing a role in active surveillance.[3,4]

Whilst being a useful rule out test with high sensitivity, specificity is not high enough to justify radical treatment without histological confirmation as other conditions can be difficult to distinguish from prostate cancer radiologically. A number of benign conditions may confound MRI interpretation and be mistaken for tumours. Normal anatomical structures, including the central zone, thickening of the surgical capsule, periprostatic venous plexus and neurovascular bundles can be mistaken for adenocarcinoma.[5] Additionally, benign abnormalities that can mimic tumour include post-biopsy haemorrhage, stromal benign prostatic hyperplasia nodules, acute and chronic prostatitis, and granulomatous prostatitis.

Granulomatous prostatitis (GP) is a benign inflammatory condition of the prostate, characterised histologically by the presence of granulomas, i.e. foci of chronic inflammation with aggregations of macrophages surrounded by a collar of mononuclear leukocytes and plasma cells.[6,7] It may be idiopathic (nonspecific) or secondary to causes including urinary tract infection (UTI), bacillus Calmette-Guérin (BCG) therapy for bladder transitional cell carcinoma (TCC), surgery, or systemic disease.[6]

GP mimics prostate cancer clinically with raised PSA and suspicious examination findings, and radiologically with hypointense signals on T_2weighted (T2w) MR imaging. However, because of its relative rarity, studies utilising contemporary mpMRI have been limited.[8,9] Identification of radiological features specific to GP may allow for easier diagnosis and reduction in patient morbidity through fewer prostate biopsies. We therefore aimed to present the mpMRI imaging findings in a series of 16 GP patients.

PATIENTS AND METHODS

Patients

We retrospectively reviewed a prospectively-collected database of males undergoing investigation for prostate adenocarcinoma. All patients at our centre routinely undergo mpMRI and transperineal sector-guided prostate biopsy (TPSB). Patients between July 2012 and May 2017 (n = 819) were reviewed. 16 patients with pathologically-proven GP were identified. All patients had undergone mpMRI in the 180 days prior to biopsy. Those with active UTI were treated with antibiotics prior to mpMRI. The reference standard for pathological diagnosis of GP was established using 24 to 40 core TPSB with additional cognitive targeting of suspicious MR lesions, as previously described.[10,11] Patients with synchronous prostate cancer and previous intravesical BCG treatment were excluded.

MR imaging

MR imaging was performed at three centres: our home institution (n = 13) and two local referral centres (Referral Centre 1, n = 2 and Referral Centre 2, n = 1). MR imaging was carried out with 1.5 Tesla machines at all centres (Home and Referral Centre 1: Signa Excite, GE Healthcare, Little Chalfont, UK and Referral Centre 2: Siemens Magnetom Symphony, Siemens AG, Munich, Germany) and 8-channel phased array body coils. MRI protocols for each centre are displayed in Table 1. DWI images were collected with b-values of 0 and 1400 at the home centre and Referral Centre 1 (n = 13), and 0 and 800 at Referral Centre 2.

Image analysis

A single radiologist (SHL), with 7 years post-training experience with prostate mpMRI, evaluated the images and recorded the following findings: tumour location, lesion shape, size, presence of extracapsular extension, signal intensity (SI) on T_2 weighted (T2w) and diffusion-weighted images (DWI), apparent diffusion

Table 1. Multiparametric MRI protocols for Home and 2 Referral Centres

Parameter	Centre	Axial T2 TSE	Sagittal T2 TSE	Coronal T2 TSE	DWI	DCE
TR (ms)	**Home**	3960	4560	3780	4975	3.3
	1	4500	6540	4300	5275	3.9
	2	3420	4610	2870	5600	-
TE (ms)	**Home**	120	120	120	82	1.6
	1	106.7	88.7	102.2	84.4	1.6
	2	99	103	103	89	-
Field of view (mm)	**Home**	200 × 200	240 × 240	200 × 200	340 × 340	230 × 230
	1	230 × 230	230 × 230	230 × 230	340 × 340	300 × 300
	2	250 × 250	220 × 220	200 × 200	267 × 267	-
Matrix size	**Home**	288 × 288	384 × 384	288 × 288	98 × 128	160 × 160
	1	288 × 256	288 × 224	320 × 256	98 × 128	192 × 192
	2	102 × 160	160 × 320	192 × 320	102 × 160	-
Slice thickness (mm)	**Home**	3	3	3	4	4 (2mm overlap)
	1	3	3	3	4	5
	2	3	3	3	3.6	-
Flip angle (°)	**Home**	90	90	90	180	12
	1	90	90	90	90	12
	2	150	150	150	-	-
Scan time (mins)	**Home**	5:09	3:16	4:55	5:03	5:38
	1	3:41	4:41	3:31	5:16	6:05
	2	4:40	2:00	3:00	9:38	-
Temporal resolution (s)	**Home**	-	-	-	-	12
	1	-	-	-	-	12
	2	-	-	-	-	-

coefficient (ADC) values, multiphase contrast enhancement pattern on dynamic contrast enhanced (DCE) images and PI-RADS (Prostate Imaging Reporting and Data System) score. PI-RADS score was reported as per the version two scoring system.[12]

SI on T2w images was determined visually, compared to femoral head bone marrow and obturator muscle. SI on DWI was compared with residual normal peripheral zone (PZ) tissue. DCE images were available for five patients with appearances and pattern evaluated based on arterial, venous and equilibrium Phase images. ADC values were calculated by placing a round region of interest (ROI) on three areas within the prostate deemed to visually have the lowest SI. The values were averaged and reported for each case.

RESULTS

In total, 16 patients with pathologically proven GP were included in the study. These consisted of 13 cases of primary, nonspecific GP (NGP) and 3 cases of xanthogranulomatous prostatitis (XGP). Median age was 62.5 (range 46–78) years. Patients were referred for either rising PSA (n = 12) or abnormal DRE (n = 4). Clinically, 12 patients had UTI treated with antibiotics prior to MRI. Median PSA was 7.7 ng ml^{-1} (range 2.2–78.7 ng ml^{-1}), median prostate volume was 46.5 ml (range 24–86 ml) and median PSA density was 0.15 ng/ml^2 (range 0.06–1.09 ng/ml^2). Patient demographics, clinical investigations and MR imaging features are summarised in Table 2.

On mpMRI, 13 GP lesions were diffuse in nature, involving the PZ and transition zone (TZ), with greater than 50% of the gland involved; one patient had a further cystic component. In these diffuse lesions, normal PZ/TZ zonal architecture was lost, and histology showed NGP (n = 12) and XGP (n = 1). The remaining three patients had nodular lesions, two within the PZ only, and one involving both the PZ and TZ. Histology in these nodular patients included NGP (n = 1) and XGP (n = 2).

Capsular irregularity suspicious for early extracapsular extension was seen in 15 patients, simulating T3a prostate adenocarcinoma. On T2w imaging, all lesions had lower signal intensity (SI) than femoral head bone marrow, and higher SI than obturator muscle. On DWI, all lesions had higher SI than normal PZ. ADC values were available for 14 patients. DWI was available for 13 patients, and characterised by low ADC values (mean ADC 702 ± 79×10^{-6} mm/s^2). DCE imaging was available in five patients. All cases had diffuse enhancement post-contrast, but two cases displayed further rim enhancement. All cases were 'positive' as per PI-RADS v2 guidelines. Overall PI-RADS v2 score for all cases was 5, indicating 'Clinically significant cancer is highly likely to be present'.[12]

We highlight salient radiological findings in four patients:

- Case 1 was a 64-year-old male referred with PSA of 10.1 ng ml^{-1} which remained elevated following successful treatment of a UTI (Figures 1–3). The images highlight the diffuse low SI on T2 and high SI on DWI, with ring enhancement on DCE.
- Case 2 was a 57-year-old gentleman who was catheterised following an episode of acute urinary retention secondary to UTI. His presenting PSA was 17.5 ng ml^{-1} (Figures 4–5). This case shows the very low ADC values attained in many GP patients.
- Case 3 was a 46-year-old male who was referred in by his primary care doctor with a PSA of 5.5 (Figure 6). This image series is an excellent example of GP extracapsular extension.
- Case 4 was a 65-year-old male presenting with an elevated PSA of 6.4 (Figure 7); this image series is an example of nodular GP.

DISCUSSION

Patients undergoing investigation for prostate cancer now routinely undergo pre-operative mpMRI. In these patients, various conditions may mimic prostate cancer. Recognition of these conditions, which may include acute and chronic prostatitis, GP, postinflammatory scars, etc., is important to reduce biopsy rates for these benign conditions.[5] GP is a benign, inflammatory condition of the prostate that is estimated to comprise 3.3% of all inflammatory prostate lesions.[13] The aetiology of nonspecific GP is unknown, but thought to arise from blockage of prostatic ducts, leading to stasis of secretions and epithelial disruption. Debris and secretion escape into surrounding stroma, leading to localised inflammatory reaction.[6]

GP lesions are benign and typically require no treatment, but are often mistaken radiologically for malignant tumours, including prostate adenocarcinoma or prostatic invasion of bladder TCC. We present an mpMRI case series of 16 GP patients, confirmed with TPSB. Of these, 13 were primary NGP with no previous BCG treatment, which is to our knowledge the largest series of mpMRI findings in NGP.

A series by Oppenheimer et al,[14] of over 25,000 males undergoing prostate biopsy, reported the incidence of GP to be 0.36%. Compared to this, our incidence of 2.0% is approximately 6-fold higher. This may be explained by the patient population. Oppenheimer identified cases from a population of patients undergoing transrectal biopsy for raised PSA or abnormal digital rectal examination. Our cohort consisted of patients undergoing mpMRI followed by systematic transperitoneal biopsies. This likely enriched the cohort, as patients were more likely to undergo biopsy if they had abnormal imaging and the greater number cores taken using systematic biopsies was more likely to identify GP.

Our findings are consistent with previous studies highlighting the radiological overlap between GP and prostate adenocarcinoma. A summary of GP mpMRI findings from this study *vs* typical prostate cancer mpMRI findings is shown in Table 3.[1,12,15] Striking findings from this study included the low ADC values in GP. ADC values are commonly lower in prostate cancer tissue versus normal prostastic tissue, with low ADC values inversely correlating with Gleason scoring.[15–19] GP lesions in our cohort have very low ADC values (mean ADC value of 702 ± 79×10^{-6} mm/s^2), similar to that seen in Gleason ≥ 8 cancers.[15,19]

Table 2. MR Imaging Features of Granulomatous Prostatitis in 8 Patients

Case	Age (yrs)	PSA (ng/ml)	Vol (ml)	Shape	Location	ECE	SI of T2WI (*vs* BM / *vs* OM)	SI of DWI (*vs* Normal PZ)	Mean ADC	PI-RADS	Previous UTI?	Histology
1	64	10.1	64	Diffuse (≥50%), Cystic	TZ PZ	+	↓ / ↑	↑	-	5	+	NGP
2	54	4.0	71	Diffuse (≥50%)	TZ PZ	+	↓ / ↑	↑	600	5	+	NGP
3	46	5.5	36	Diffuse (≥50%)	TZ PZ	+	↓ / ↑	↑	604	5	+	NGP
4	65	6.4	32	Nodular	TZ PZ	+	↓ / ↑	↑	666	5	+	XGP
5	58	17.5	64	Diffuse (≥50%)	TZ PZ	+	↓ / ↑	↑	695	5	+	NGP
6	52	6.7	50	Diffuse (≥50%)	TZ PZ	+	↓ / ↑	↑	-	5	-	NGP
7	65	16.9	41	Diffuse (≥50%)	TZ PZ	+	↓ / ↑	↑	797	5	+	NGP
8	48	2.24	24	Diffuse (≥50%)	TZ PZ	+	↓ / ↑	↑	642	5	-	NGP
9	71	3.19	37	Nodular	PZ	+	↓ / ↑	↑	-	5	+	NGP
10	67	9.33	86	Diffuse (≥50%)	TZ PZ	+	↓ / ↑	↑	660	5	+	NGP
11	67	6.5	43	Diffuse (≥50%)	TZ PZ	+	↓ / ↑	↑	811	5	+	XGP
12	61	78.7	72	Diffuse (≥50%)	TZ PZ	+	↓ / ↑	↑	666	5	-	NGP
13	46	2.8	35	Diffuse (≥50%)	TZ PZ	+	↓ / ↑	↑	667	5	+	NGP
14	56	13.0	26	Diffuse (≥50%)	TZ PZ	-	↓ / ↑	↑	720	5	-	NGP
15	78	8.7	65	Diffuse (≥50%)	TZ PZ	+	↓ / ↑	↑	853	5	+	NGP
16	74	37.3	69	Nodular	PZ	+	↓ / ↑	↑	744	5	+	XGP

PSA = Prostate Specific Antigen, ECE = Extracapsular Extension, TZ = Transition Zone, PZ = Peripheral Zone, SI = Signal Intensity, T2WI = T_2 weighted2 weighted, BM = Bone Marrow, OM = Obturator Muscle, ADC = apparent diffusion coefficient, PI-RADS = Prostate Imaging Reporting and Data System, UTI = Urinary Tract Infection, NGP = Nonspecific Granulomatous Prostatitis, BCG-GP = Bacillus Calmette Guérin-induced Granulomatous Prostatitis, XGP = Xanthogranulomatous Prostatitis

Figure 1. Case 1: Coronal T2WI and axial T2WI, DWI (b-value 1400) and ADC maps at the levels of prostate base (A), mid gland (B) and apex (C), demonstrating diffuse low T2 SI in the PZ and TZ and interspersed by multifocal areas of high T2 SI (asterisk). These areas show high SI on the DWI and very low SI on the ADC maps resulting in a PI-RADS score of 5.

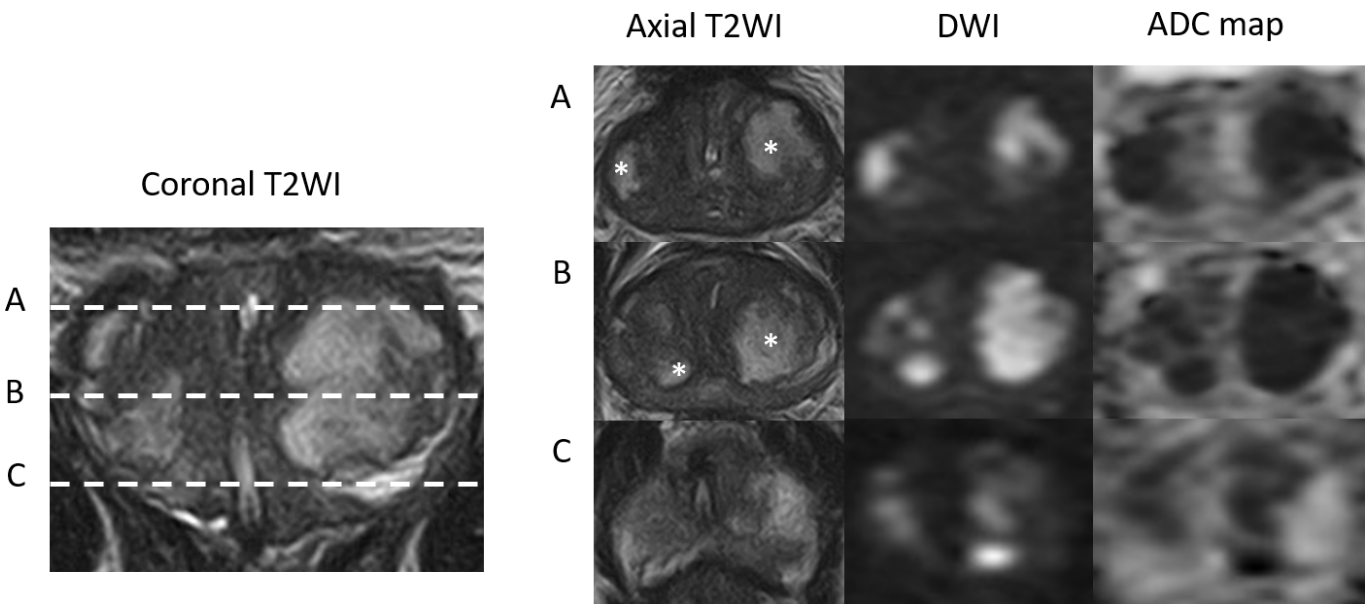

Additionally, ring enhancement on DCE sequences may aid diagnosis in certain cases but is dependent on caseation and abscess formation, often absent in nonspecific GP. Patients scanned early in the disease process may not demonstrate this radiological feature.[20] A high proportion of patients had pre-mpMRI UTIs which were treated with antibiotics prior to their imaging being performed. In these patients, radiologists must have a high index of suspicion for GP.

The PI-RADS system is most commonly used to score prostate mpMRIs.[12] These guidelines for prostate mpMRI include minimal and optimal acquisition protocols, and a structured category assessment for radiologists. Within this series, GP lesions were highly suspicious of prostate cancer based on this scoring system. This is unsurprising given the known overlap between GP and prostate cancer, particularly on T2 and DWI sequences. At present, use of PI-RADS contributes little to diagnosis of GP based on mpMRI findings.

Rais-Bahrami et al[21] reported their mpMRI findings of 5 GP cases matched to 15 Gleason ≥4 +3 prostate cancer cases. Of these, two patients had received prior intravesical BCG treatment. Mean ADC values were higher for the GP cases *vs* the prostate cancer (mean 1051.0 *vs* 791.7 × 10^{-6} mm/s^2). This lies in contrast to the values seen in this series, and is of particular interest as 4 out of 5 cases were found to have synchronous prostate cancer. It is unclear as to how this additional prostate cancer influenced underlying ADC values, particularly as GP was only detected on MRI-targeted cores, and not systematic biopsies.

Figure 2. Case 1: DCE axial images obtained in arterial (A), venous (B) and equilibrium (C) phases, showing multifocal areas of early and prolonged ring enhancement;

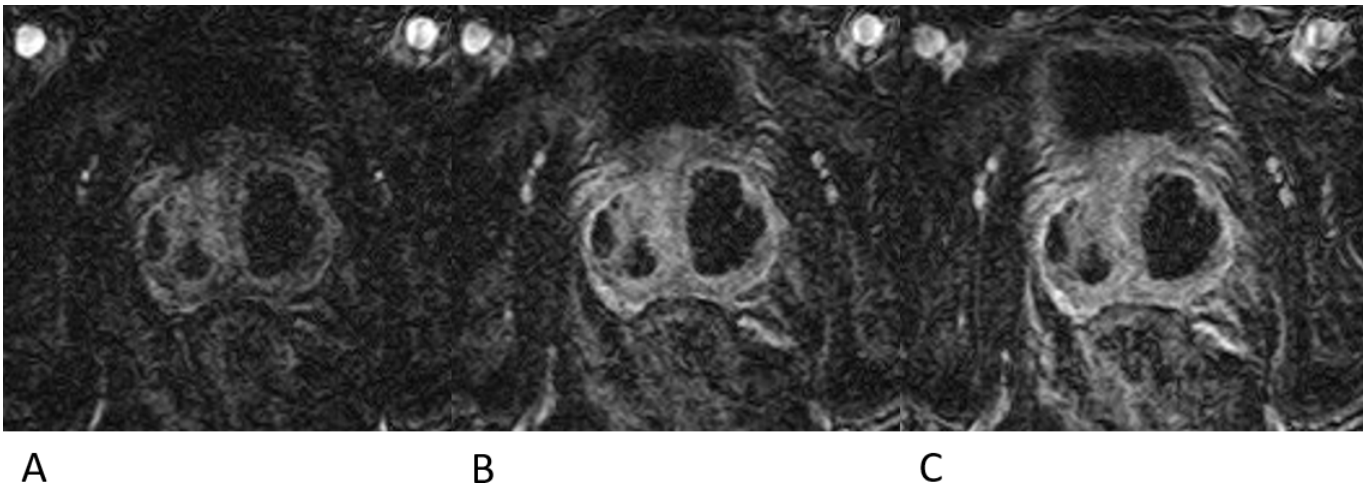

Figure 3. Case 1: Coronal T2WI (A), axial T2WI (B), DWI (b-value 1400) (C) and ADC map (D) obtained 6 months after the initial MRI and following a prolonged course of antibiotics (ciprofloxacin). There is reconstitution of normal prostate zonal anatomy and high T2 SI of the PZ. There are no areas of restricted water diffusion on the DWI and ADC map.

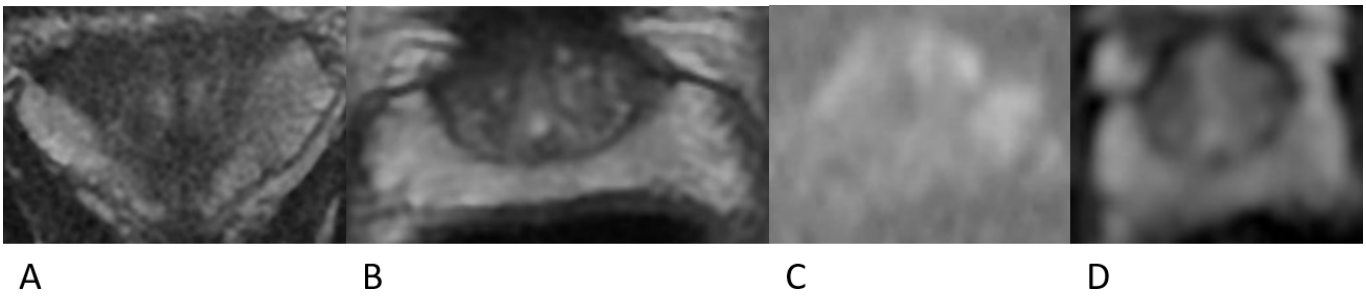

No GP case in the Rais-Bahrami series displayed imaging suspicious of higher stage disease, but was seen in a third of the prostate cancer patients.[21] The authors suggest that lower ADC values in the absence of higher stage features may suggest GP over prostate cancer. These contrast to our series, particularly as the majority of these patients also displayed extracapsular extension, predominantly as a capsular bulge. This may have arisen from the diffuse nature of GP disease in this series, with the inflammation causing this capsular bulge.

Earlier studies reviewed MRI findings in patients suffering from BCG-induced GP, giving the incidence following intravesical BCG to be as high as 41%.[22,23] These had similar findings of markedly low T2w SI, with no clear GP imaging pattern.[9,24] Kawada et al[8] showed early and prolonged ring enhancement on DCE sequences corresponded to caseous necrosis in BCG-induced GP. Bour et al[25] described two patterns of GP MRI appearance: first, the frequently reported tumour-like appearance that cannot be distinguished from prostate cancer, and second, a rarer appearance corresponding to caseous necrosis and abscess formation, as per Kawada et al. Finally, Gottlieb et al[26] also described two patterns: circumscribed lesions with low ADC values and isointense signal on high b-value DWI, or non-circumscribed lesions with decreased ADC and high SI on DWI, consistent with restricted diffusion and indistinguishable from prostate cancer. All these studies were based on small series of BCG-induced GP, but highlight varying imaging patterns in GP. It is unclear if these findings overlap with primary NGP. Given the high incidence of GP following intravesical BCG, radiologists should be provided with a clear clinical history.

This study benefits from the use of specific prostate mpMRI sequences. Many previous series have used MRI to assess

Figure 4. Case 2: Coronal T2WI and axial T2WI, DWI (b-value 1400) and ADC maps at the level of prostatic base (A), mid gland (B) and apex (C), demonstrating diffuse low T2 SI in the PZ and TZ with a small area of preserved normal SI in the right posteromedial PZ (arrowhead). The majority of the prostate is high in SI on the DWI and low in SI on the ADC map resulting in a PI-RADS score of 5. There is an indwelling Foley catheter *in situ* (asterisk).

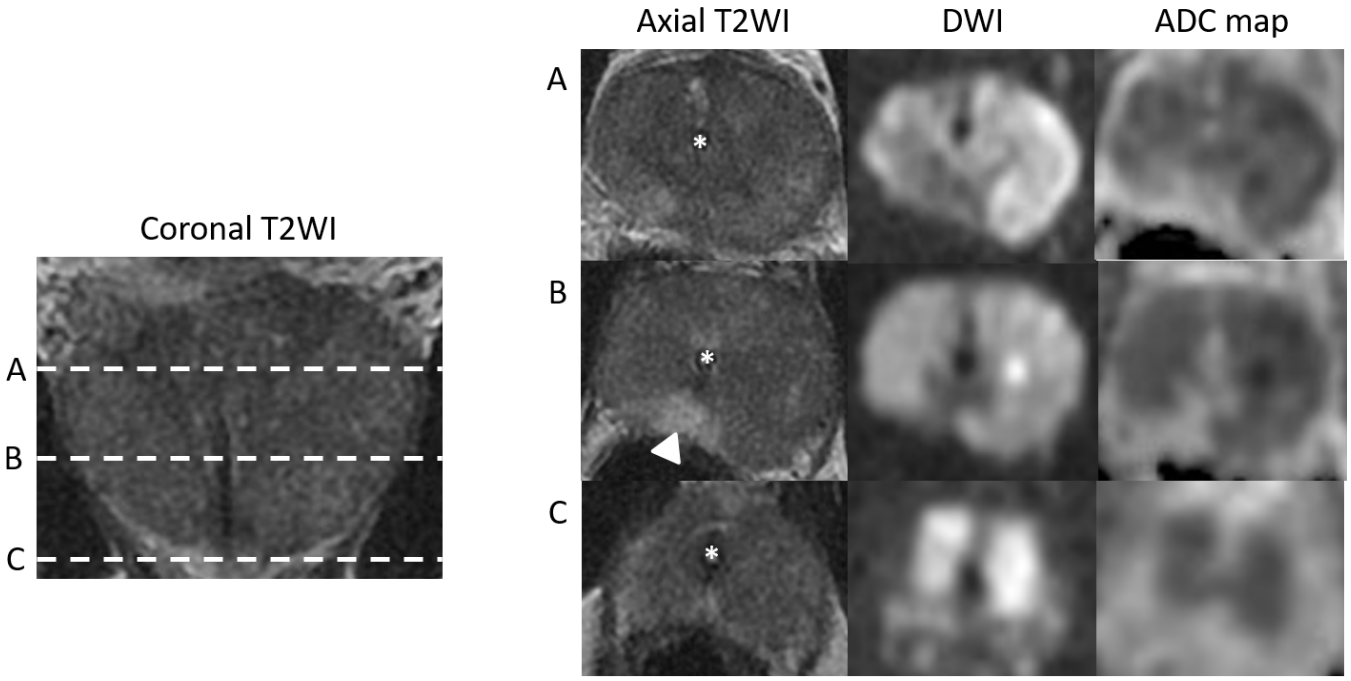

Figure 5. Case 2: ADC map showing the ADC values (10^{-6} mm^2/s) for three ROIs placed in the spared posteromedial right PZ (circle 1 – ADC value 1686) and in two areas of very low SI on the ADC map (circle 2 – ADC value 792 and circle 3 – ADC value 752) indicating marked restricted water diffusion.

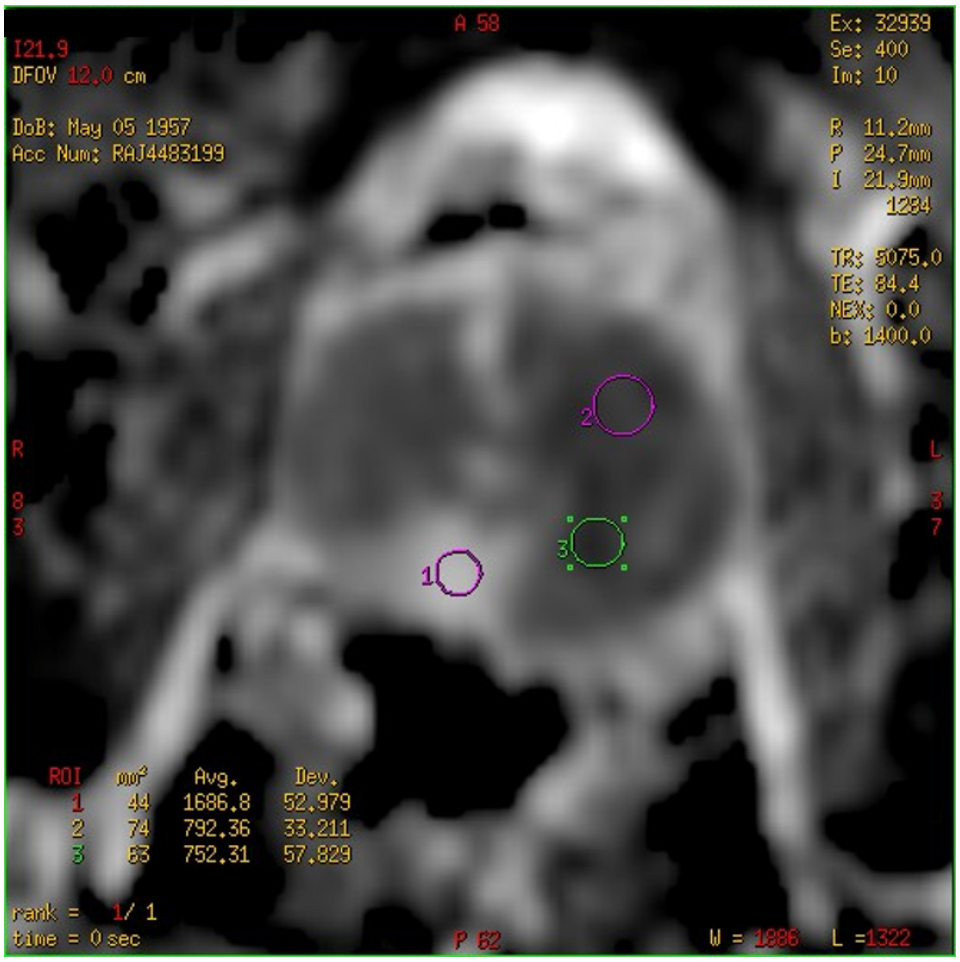

Figure 6. Case 3: Coronal T2WI and corresponding axial T2WI, DWI (b-value 1400), ADC maps and DCE images at the levels of prostatic base (A), mid gland (B) and apex (C), demonstrating diffuse low T2 SI in the PZ and TZ with a small area of relatively preserved normal SI in the posterior apical PZ (asterisk). The majority of the prostate is high in SI on the DWI and low in SI on the ADC map and shows diffuse hyperenhancement on DCE. This results in a PI-RADS score of 5 for both T2WI and DWI and positive for DCE (PI-RADS v2). Note the area of capsular bulging in the right posterior apex (arrow).

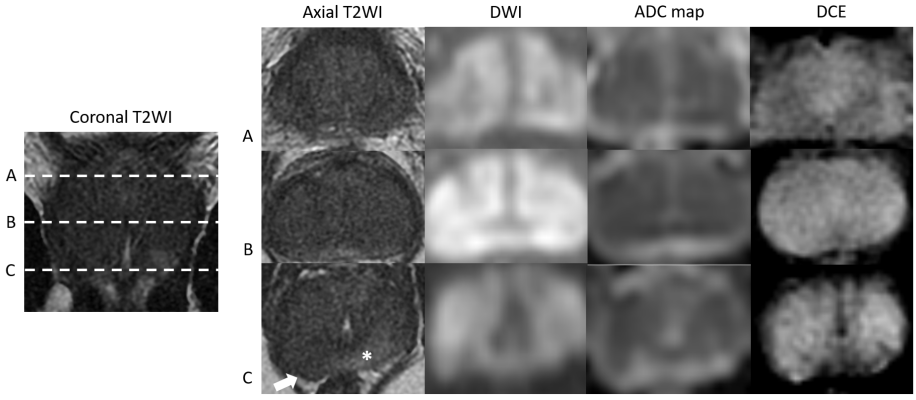

Figure 7. Case 4: Axial T2WI (a) , DWI (B) , ADC map (C) and DCE (D)images demonstrating a large (>1.5 cm) nodular low T2SI in the right basal PZ with marked focal restricted diffusion (ADC value 634) and asymmetrical focal enhancement (PI-RADS v2 5/5). (E) DCE image in the same patient at the mid gland level shows a focal area of hypo or rim enhancement (arrow) thought to represent an area of preserved normal PZ.

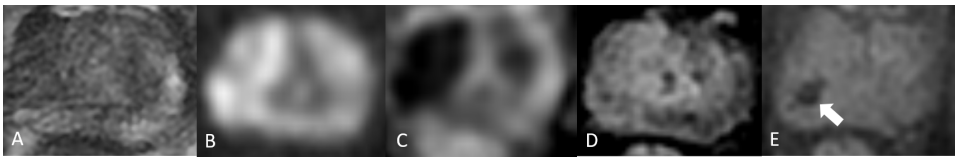

Table 3. Comparison of MRI findings for Granulomatous Prostatitis and Prostate Cancer

Sequence	Granulomatous Prostatitis	Prostate Cancer
T2	• Diffuse or nodular pattern • Low signal intensity lesions • Loss of normal peripheral zone/transitional zone architecture • May show capsular irregularity, suggestive of high stage prostate cancer	• Round or ill-defined, low signal intensity focus in peripheral zone. • May appear as lenticular or homogeneous signal mass with indistinct margins ("erased charcoal sign") in transitional zone. • Higher grade cancers often have lower signal intensity than low grade tumours.
DWI	• High signal intensity on DWI • Very low ADC values compared to normal normal peripheral zone tissue (mean ADC 702 ± 79×10^{-6} mm/s^2).	• High signal intensity on DWI • Low ADC values compared to normal peripheral zone tissue. • ADC values inversely correlate with increasing Gleason score. Lowest values seen in Gleason > 8 cancers.
DCE	• Early diffuse enhancement seen in all cases. • A subset of patients have rim enhancement, consistent with caseous necrosis and abscess formation.	• Prostate cancer may reveal early and increased enhancement • Lack of enhancement does not exclude malignancy • Best used to discriminate equivocal lesions in the peripeheral zone.

bladder cancer staging and performance of BCG therapy.[8,24,25] Furthermore, patients underwent systematic, sector-guided transperineal prostate biopsies, allowing for diagnosis of GP and exclusion of synchronous cancer.[11] Pathological diagnosis was not available for all cases in certain prior GP studies.[25]

We do recognise study limitations. This study was retrospective, and as all patients were investigated for prostate cancer, we are unable to comment on prevalence of GP and potential mpMRI findings of subclinical GP. We chose to exclude any cases with concurrent prostate cancer and previous intravesical BCG history, to delineate the appearances of GP without overlap from these associated conditions.

It is important to note the cases of XGP. XGP is a rare form of GP, which is histologically similar, but with prominent foamy histiocytes.[9,27] Findings can be consistent between NGP and this subtype, including diffuse lesions and low ADC values, but we cannot draw comparisons on the basis of three cases. Finally, this study comprised mpMRI scans from three institutions; DCE imaging was available for only five patients. For DWI sequences, these were only available for the home institution. However, these values were consistently low for GP lesions across these patients.

CONCLUSION

Distinguishing GP from prostate cancer on MR imaging remains a challenge, but certain features may help guide diagnosis and decision-making. GP may present as diffuse MRI lesions involving the PZ and TZ and >50% of the gland with appearances of extracapsular extension and rim-enhancing areas. It should remain a differential diagnosis when these features are present, particularly in patients with recent UTI or BCG therapy. However, biopsy is still necessary as imaging features are not definitive.

REFERENCES

1. Barentsz JO, Richenberg J, Clements R, Choyke P, Verma S, Villeirs G, et al. ESUR prostate Mr guidelines 2012. *Eur Radiol* 2012; **22**: 746–57. doi: https://doi.org/10.1007/s00330-011-2377-y
2. Fütterer JJ, Briganti A, De Visschere P, Emberton M, Giannarini G, Kirkham A, et al. Can clinically significant prostate cancer be detected with multiparametric magnetic resonance imaging? A systematic review of the literature. *Eur Urol* 2015; **68**:

1045–53. doi: https://doi.org/10.1016/j.eururo.2015.01.013
3. Grey ADR, Chana MS, Popert R, Wolfe K, Liyanage SH, Acher PL. Diagnostic accuracy of magnetic resonance imaging (MRI) prostate imaging reporting and data system (PI-RADS) scoring in a transperineal prostate biopsy setting. *BJU Int* 2015; **115**: 728–35. doi: https://doi.org/10.1111/bju.12862
4. Schoots IG, Petrides N, Giganti F, Bokhorst LP, Rannikko A, Klotz L, et al. Magnetic resonance imaging in active surveillance of prostate cancer: a systematic review. *Eur Urol* 2015; **67**: 627–36. doi: https://doi.org/10.1016/j.eururo.2014.10.050
5. Rosenkrantz AB, Taneja SS, Radiologist TSS. Radiologist, be aware: ten pitfalls that confound the interpretation of multiparametric prostate MRI. *AJR Am J Roentgenol* 2014; **202**: 109–20. doi: https://doi.org/10.2214/AJR.13.10699
6. Srigley JR. Benign mimickers of prostatic adenocarcinoma. *Mod Pathol* 2004; **17**: 328–48. doi: https://doi.org/10.1038/modpathol.3800055
7. James DG. A clinicopathological classification of granulomatous disorders. *Postgrad Med J* 2000; **76**: 457–65. doi: https://doi.org/10.1136/pmj.76.898.457
8. Kawada H, Kanematsu M, Goshima S, Kondo H, Watanabe H, Noda Y, et al. Multiphase contrast-enhanced magnetic resonance imaging features of Bacillus Calmette-Guérin-induced granulomatous prostatitis in five patients. *Korean J Radiol* 2015; **16**: 342–8Apr. doi: https://doi.org/10.3348/kjr.2015.16.2.342
9. Suzuki T, Takeuchi M, Naiki T, Kawai N, Kohri K, Hara M, et al. MRI findings of granulomatous prostatitis developing after intravesical Bacillus Calmette-Guérin therapy. *Clin Radiol* 2013; **68**: 595–9. doi: https://doi.org/10.1016/j.crad.2012.12.005
10. Kuru TH, Wadhwa K, Chang RTM, Echeverria LMC, Roethke M, Polson A, et al. Definitions of terms, processes and a minimum dataset for transperineal prostate biopsies: a standardization approach of the Ginsburg Study Group for enhanced prostate diagnostics. *BJU Int* 2013; **112**: 568–77. doi: https://doi.org/10.1111/bju.12132
11. Vyas L, Acher P, Kinsella J, Challacombe B, Chang RTM, Sturch P, et al. Indications, results and safety profile of transperineal sector biopsies (TpsB) of the prostate: a single centre experience of 634 cases. *BJU Int* 2014; **114**: 32–7. doi: https://doi.org/10.1111/bju.12282
12. Weinreb JC, Barentsz JO, Choyke PL, Cornud F, Haider MA, Macura KJ, et al. PI-RADS Prostate Imaging - Reporting and Data System: 2015, Version 2. *Eur Urol* 2016; **69**: 16–40. doi: https://doi.org/10.1016/j.eururo.2015.08.052
13. Mohan H, Bal A, Punia RPS, Bawa AS. Granulomatous prostatitis--an infrequent diagnosis. *Int J Urol* 2005; **12**: 474–8. doi: https://doi.org/10.1111/j.1442-2042.2005.01068.x
14. Oppenheimer JR, Kahane H, Epstein JI. Granulomatous prostatitis on needle biopsy. *Arch Pathol Lab Med* 1997; **121**: 724–9.
15. Yu AC, Badve C, Ponsky LE, Pahwa S, Dastmalchian S, Rogers M, et al. Development of a combined Mr fingerprinting and diffusion examination for prostate cancer. *Radiology* 2017; **283**: 729–38. doi: https://doi.org/10.1148/radiol.2017161599
16. Afaq A, Koh D-M, Padhani A, van As N, Sohaib SA. Clinical utility of diffusion-weighted magnetic resonance imaging in prostate cancer. *BJU Int* 2011; **108**: 1716–22. doi: https://doi.org/10.1111/j.1464-410X.2011.10256.x
17. De Cobelli F, Ravelli S, Esposito A, Giganti F, Gallina A, Montorsi F, et al. Apparent diffusion coefficient value and ratio as noninvasive potential biomarkers to predict prostate cancer grading: comparison with prostate biopsy and radical prostatectomy specimen. *AJR Am J Roentgenol* 2015; **204**: 550–7. doi: https://doi.org/10.2214/AJR.14.13146
18. Lebovici A, Sfrangeu SA, Feier D, Caraiani C, Lucan C, Suciu M, et al. Evaluation of the normal-to-diseased apparent diffusion coefficient ratio as an indicator of prostate cancer aggressiveness. *BMC Med Imaging* 2014; **14**: 15. doi: https://doi.org/10.1186/1471-2342-14-15
19. Turkbey B, Shah VP, Pang Y, Bernardo M, Xu S, Kruecker J, et al. Is apparent diffusion coefficient associated with clinical risk scores for prostate cancers that are visible on 3-T MR images? *Radiology* 2011; **258**: 488–95. doi: https://doi.org/10.1148/radiol.10100667
20. Presti B, Weidner N. Granulomatous prostatitis and poorly differentiated prostate carcinoma. Their distinction with the use of immunohistochemical methods. *Am J Clin Pathol* 1991; **95**: 330–4. doi: https://doi.org/10.1093/ajcp/95.3.330
21. Rais-Bahrami S, Nix JW, Turkbey B, Pietryga JA, Sanyal R, Thomas JV, et al. Clinical and multiparametric MRI signatures of granulomatous prostatitis. *Abdom Radiol* 2017; **42**: 1956–62. doi: https://doi.org/10.1007/s00261-017-1080-0
22. Lamm DL, Stogdill VD, Stogdill BJ, Crispen RG. Complications of Bacillus Calmette-Guerin immunotherapy in 1,278 patients with bladder cancer. *J Urol* 1986; **135**: 272–4. doi: https://doi.org/10.1016/S0022-5347(17)45606-0
23. Oates RD, Stilmant MM, Freedlund MC, Siroky MB. Granulomatous prostatitis following Bacillus Calmette-Guerin immunotherapy of bladder cancer. *J Urol* 1988; **140**: 751–4. doi: https://doi.org/10.1016/S0022-5347(17)41803-9
24. Naik KS, Carey BM. The transrectal ultrasound and MRI appearances of granulomatous prostatitis and its differentiation from carcinoma. *Clin Radiol* 1999; **54**: 173–5. doi: https://doi.org/10.1016/S0009-9260(99)91009-7
25. Bour L, Schull A, Delongchamps N-B, Beuvon F, Muradyan N, Legmann P, et al. Multiparametric MRI features of granulomatous prostatitis and tubercular prostate abscess. *Diagn Interv Imaging* 2013; **94**: 84–90. doi: https://doi.org/10.1016/j.diii.2012.09.001
26. Gottlieb J, Princenthal R, Cohen MI. Multiparametric MRI findings of granulomatous prostatitis developing after intravesical Bacillus calmette–guérin therapy. *Abdom Radiol* 2017; **42**: 1963–7. doi: https://doi.org/10.1007/s00261-017-1081-z
27. Pastore AL, Palleschi G, Fuschi A, Porta N, Cerbelli B, Di Cristofano C, et al. Hematospermia and xanthogranulomatous prostatitis: an unusual onset of a rare diagnosis. *Can Urol Assoc J* 2013; **7**(11-12): 820–2Dec. doi: https://doi.org/10.5489/cuaj.1525